Biomaterials 181 (2018) 392–401

Contents lists available at ScienceDirect

Biomaterials

journal homepage: www.elsevier.com/locate/biomaterials

Thermosensitive biomimetic polyisocyanopeptide hydrogels may facilitate wound repair

Roel C. op 't Veld [a, c], Onno I. van den Boomen [b], Ditte M.S. Lundvig [c], Ewald M. Bronkhorst [d], Paul H.J. Kouwer [b], John A. Jansen [a], Esther Middelkoop [e, f], Johannes W. Von den Hoff [c], Alan E. Rowan [b], Frank A.D.T.G. Wagener [c, *]

[a] Department of Biomaterials, Radboud Institute for Molecular Life Sciences, Radboud university medical center, Nijmegen, The Netherlands
[b] Department of Molecular Materials, Institute for Molecules and Materials, Radboud University, Nijmegen, The Netherlands
[c] Department of Orthodontics and Craniofacial Biology, Radboud Institute for Molecular Life Sciences, Radboud university medical center, Nijmegen, The Netherlands
[d] Department of Cariology and Preventive Dentistry, Radboud Institute for Molecular Life Sciences, Radboud university medical center, Nijmegen, The Netherlands
[e] Association of Dutch Burn Centres, Martini Hospital, Groningen, The Netherlands
[f] Department of Plastic, Reconstructive and Hand Surgery, Amsterdam Movement Sciences, VU University Medical Centre, Amsterdam, The Netherlands

ARTICLE INFO

Article history:
Received 9 April 2018
Received in revised form
20 July 2018
Accepted 25 July 2018
Available online 30 July 2018

Keywords:
Hydrogel
Polyisocyanopeptide
Wound repair
Biomimetic
Mesoporous

ABSTRACT

Changing wound dressings inflicts pain and may disrupt wound repair. Novel synthetic thermosensitive hydrogels based on polyisocyanopeptide (PIC) offer a solution. These gels are liquid below 16 °C and form gels beyond room temperature. The architecture and mechanical properties of PIC gels closely resemble collagen and fibrin, and include the characteristic stiffening response at high strains. Considering the reversible thermo-responsive behavior, we postulate that PIC gels are easy to apply and remove, and facilitate healing without eliciting foreign body responses or excessive inflammation. Biocompatibility may be higher in RGD-peptide-functionalized PIC gels due to enhanced cell binding capabilities. Full-thickness dorsal skin wounds in mice were compared to wounds treated with PIC gel and PIC-RGD gel for 3 and 7 days. No foreign body reactions and similar wound closure rates were found in all groups. The level of macrophages, myofibroblasts, epithelial migration, collagen expression, and blood vessels did not significantly differ from controls. Surprisingly, granulocyte populations in the wound decreased significantly in the PIC gel-treated groups, likely because foreign bacteria could not penetrate the gel. RGD-peptides did not further improve any effect observed for PIC. The absence of adverse effects, ease of application, and the possibilities for bio-functionalization make the biomimetic PIC hydrogels suitable for development into wound dressings.

1. Introduction

Cutaneous injury as a result of burns, surgery, or trauma may lead to severe scar formation and impaired functionality [1]. Following injury, diverse processes are activated to minimize hemorrhage, to destroy infectious agents, debride the wound of dead tissue, and, finally, to promote tissue repair and regeneration [2]. Many different cell types are involved in the repair process of wounds.

The wound repair process can be roughly characterized by four distinct phases: hemostasis, inflammation, proliferation, and remodeling. First, a blood clot is formed, wherein recruited activated platelets crosslink polymerized fibrin to form a hemostatic plug. During the inflammatory phase granulocytes and macrophages are recruited into the wound area to kill invading pathogens and remove debris [3,4]. The proliferation phase mediates tissue repair, including wound epithelialization, angiogenesis, and wound contraction. Keratinocytes migrate from the wound edge to re-epithelialize the complete wound area, while new blood vessels are organized into a microvascular network supporting the forming granulation tissue. Recruited fibroblasts deposit extracellular matrix (ECM) components to provide a provisional meshwork that

* Corresponding author. Department of Orthodontics and Craniofacial Biology, Radboud university medical center, PO Box 9101, 6500HB, Nijmegen, The Netherlands.
E-mail address: Frank.Wagener@radboudumc.nl (F.A.D.T.G. Wagener).

https://doi.org/10.1016/j.biomaterials.2018.07.038
0142-9612/

helps rebuilding the injured tissue. In addition, fibroblasts differentiate into myofibroblasts that via their expression of alpha smooth muscle actin (αSMA) are able to contract in order to achieve wound closure. During the subsequent matrix remodeling phase re-arrangement of the disorganized ECM meshwork takes place, resulting in a stronger fiber network. Myofibroblasts and blood vessels that are no longer needed in the granulation tissue disappear by apoptosis, typically leaving a negligible cellularized scar.

Pathological wound repair, fueled by oxidative stress and inflammation, prevents apoptosis of myofibroblasts, leading to continued wound contraction and ECM deposition, fibrosis and excessive scar formation [1]. To facilitate the wound repair process, and to promote a good healing outcome, a wound dressing may be applied. The purpose of wound dressings is to provide protection to the wound and to maintain a micro-environment that benefits healing [5,6]. Unfortunately, the current wound dressings are not ideal as they typically need to be changed regularly, resulting in a painful "ripping open" of the wound area which will interfere with tissue repair. There is therefore an urgent need to explore novel dressings that do not hamper wound repair, but attenuate excessive scar formation and prevent cosmetic and functional problems. Ideally, a wound dressing should maintain a moist environment for optimal outgrowth of epithelial cells and provide protection against invading pathogens. Moreover, it should be easily applied, fixated and removed without causing pain, disruption or additional damage to the regenerating wound area.

Hydrogels are a prime example of modern wound dressings meant to overcome some of these issues. These products are rich in water and hydrate the wound, stimulating wound repair [7]. Yet, they still enable absorption to drain exudates. Different types of hydrogel materials exist, many of which offer additional functionalities such as acting as a scaffold or the delivery of drugs [8–13]. It is unfortunate that even with these modernized dressings complications of wound healing, such as scarring, are still rampant. A new product is desirable that is easy to apply and remove, and may offer new opportunities in the treatment of complicated wounds.

Recently, a novel thermosensitive hydrogel based on oligo(-ethylene glycol)-decorated polyisocyanopeptide (PIC) has been reported [14–16]. The gel mimics the fibrous structure and the mechanical properties of natural ECM materials [14,15,17]. Gel formation is induced by heating a polymer solution beyond its gelation temperature Tgel = 20 °C. Cooling the gel below 20 °C reverses the process and returns the polymer solution. As a result of their fibrous and porous structure and low concentrations, PIC-based hydrogels are soft, but their stiffness increases as the materials are deformed or stressed [14,15,17]. This process, called strain stiffening is also found in gels based on biopolymers, like actin and collagen, both major components of the ECM that orchestrates cell motility and differentiation. Mechanical forces can influence signal transduction, gene expression, and differentiation of cells in the wound and plays an important role in both the formation and prevention of fibrosis [18,19]. Therefore, it is desirable for a (temporary) replacement matrix to display a mechanical stiffness that mimics the natural unwounded skin and responds in a similar manner to mechanical forces such as stretch or shear. As such, the PIC gel may function as a readily removable replacement scaffold for the ECM structures that were lost upon wounding. Functionalizing biomaterials with the Arg-Gly-Asp peptide (arginyl-glycyl-aspartic acid, abbreviated to RGD or GRGDS), a ligand for integrins, enhances cell binding, bio-compatibility [20–22] and faster epithelial migration in burn wounds [23,24]. PIC gels can be readily functionalized with RGD or other molecules at the terminus of the ethylene glycol groups, which can be a strategy for improving biocompatibility or adding other functionalities [25–28].

We postulate that PIC gels are easy to apply to wounds, relying solely on body heat to achieve *in situ* gelation. Since the PIC gel mimics the extracellular microenvironment, we hypothesize that it mediates tissue integrity and homeostasis without excessive toxicity, foreign body responses and inflammation. In the present study, we investigate the *in vivo* short-term biocompatibility of the novel PIC and RGD-conjugated PIC hydrogels and their effects on wound repair in a full-thickness excisional wound model in mice.

2. Materials and methods

2.1. Synthesis of the novel biomaterials: PIC and RGD-conjugated PIC hydrogel

The synthetic gels are composed of polyisocyanopeptides with polymer backbones in a β-helical conformation that is stabilized by a peptidic hydrogen bond network. The polymers were synthesized as described previously [16]. The synthesis of RGD-functionalized PIC is summarized in Supplementary Fig. 1, and was previously reported by Das et al. [26]. The obtained polymers were characterized by viscometry (to measure Viscosity Average Molecular Weight (Mv) and estimate polymer length). For gel formation, MilliQ water or a sterile saline solution (0.9% NaCl) was added to the sterile solid polymer to reach the desired PIC concentration. After soaking for 2 h at 4 °C, the mixture was shaken vigorously for a few seconds and a clear solution was obtained. Rheology (1.6 mg/ml in MilliQ) was used to measure the gelation temperature and the storage modulus G' (gel stiffness) of the gel (see Table 1). For the animal study (3 mg/ml in saline solution), the PIC gels were taken up in a 1 ml syringe after full dissolution, quickly frozen in liquid nitrogen and placed on dry ice.

2.2. Rheology and viscometry measurements

Rheological measurements were performed on a stress-controlled rheometer (DHR-1 or DHR-2, TA-Instruments) using a steel parallel plate geometry with a diameter of 40 mm and a gap of 760 μm. All samples were loaded into the rheometer as cold polymer solutions (T = 5 °C). The mechanical properties were determined while heating the sample at a rate of 1.0 °C/min, measuring the storage and loss moduli at an oscillatory deformation of amplitude $\gamma = 0.04$ at frequency of $\omega = 1.0$ Hz. The gelation temperature was determined as the onset of the increase in storage modulus G'. Viscometry was performed as previously described [15,30].

2.3. Animals

The Committee for Animal Experiments of Radboud University Nijmegen approved all procedures involving mice (RU-DEC 2012–196 (Matrigel® pilot); RU-DEC 2013–138 (PIC gel experiments)) to conform to EU directive 2016/63/EU. For the pilot experiment six female mice (strain HO-2WT (+/+) as was previously described [31]), 8 weeks of age, and for the main study thirty-six female mice (strain: C57BL/6n, Charles River, Germany), 8 weeks of age, were used and provided with food and water *ad libitum*. Mice were maintained in groups on a 12-h light/dark cycle and specific pathogen-free housing conditions at the Central Animal Facility Nijmegen.

2.4. Full-thickness excisional wound model

Mice were anesthetized using an evaporated isoflurane/air mixture after which two full-thickness excisional wounds were created on the shaven dorsum of the mice as previously described [32].

In brief, two excisional wounds were created using a sterile

Table 1
Physical properties obtained through rheological and viscometric characterization of PIC and PIC-RGD polymers.

	M_v	n	L (nm)	G' @ 37 °C (kPa)[b]	T_{gel} (°C)[b]
PIC	613	1937	228	0.20	~15
PIC-GRGDS	652[a]	2061	242	0.23	~16

M_v: Viscosity average molecular weight as determined by viscometry; n: degree of polymerization as calculated from M_v; L: contour length calculated from M_v. The calculated polymer contour length is based on the dimensions of the polymer assuming an identical helical pitch of 0.47 nm [29]. G': Storage modulus; T_{gel}: Gelation temperature.

[a] M_v was determined from the azide intermediate since PIC-RGD does not dissolve in acetonitrile and structurally differs from non-functionalized PIC.

[b] 1.6 mg/ml MilliQ.

disposable 4-mm skin biopsy punch (Kai Medical, Seki City, Japan) on the dorsum to either side of the midline, and halfway between the shoulders. Punched out skin tissue at day 0 was collected as normal skin control (data not shown). Using this method little to no bleeding is normally observed, allowing immediate treatment.

In the pilot experiment one wound was left uncovered and one wound was covered with ~20 μl Matrigel® (10 mg/ml, BD Bioscience, Bedford, MA), a natural thermosensitive hydrogel material. At day 3 (n = 2) and day 7 (n = 4) after wounding mice were sacrificed and wounded skin was harvested.

In the following experiments, mice were randomly divided over three experimental groups. All mice received two full-thickness wounds and additional treatment according to their group. Group 1: control without gel (n = 12). Group 2: treated with a single dose (50 μl) of PIC gel to each wound (n = 12). Group 3: treated with a single dose of PIC-RGD gel (50 μl) to each wound (n = 12). Gel syringes were kept on ice and applied in the cold soluble-state. Animals were allowed to recover immediately after gelation of the gel was observed. No other bandages or dressings were used, and animals were housed in groups for the entirety of the experiment. At day 3 following wounding 6 mice of each group were sacrificed according a standard CO_2 inhalation protocol, while the remaining mice (n = 6/group) were further monitored until day 7. Control skin and wounded skin were collected using a disposable 6-mm biopsy punch (Kai Medical) allowing collection of the complete wound together with the surrounding tissue. The tissue was fixed for 24 h in 4% paraformaldehyde at room temperature, and then embedded in paraffin.

2.5. Wound size analysis

Photographs of all wounds were taken immediately after surgery, as well as after application of the hydrogel dressings with a reference ruler placed perpendicular to the wounds for measuring the wound size. Additional photographs were taken every day thereafter. Using ImageJ software (v1.44p) the surface area of the wounds of each mouse was measured on every day [33]. The size of the wounds compared to day 0 was calculated as a percentage, and the mean was calculated for replicate wounds on the same mouse.

2.6. (Immuno-)histochemical staining

Paraffin sections from both the pilot and main study were stained with azocarmine G and aniline blue (AZAN) to stain for connective tissue/collagen (blue) and other tissue structures (red) [34,35] and with haematoxylin-eosin (HE) to analyse for the presence of multinuclear giant cells, inflammatory cells, ECM components, epithelial migration, and for general morphology [36]. The migration of epithelial cells into the healing wound was scored on a scale of 0–4 (no migration (0), partial migration (1), complete migration with no/partial keratinization (2), complete migration with complete keratinization (3), and advanced hypertrophy (4)) in three representative sections of the centre of the wound, as previously described by Yates et al. [37]. All scorings in this study were performed by two assessors (RCV, FADTGW) independently of each other and then finally calculated as an average of the two. The same sections were inspected for the presence of giant cells, which were manually counted.

Immuno-histochemical stainings for macrophages (F4/80), granulocytes (GR-1) and myofibroblasts (α-SMA) were performed on paraffin sections of the wounds from the main study as previously described [32]. In short, paraffin-embedded tissues were cut into 5-μm sections, which were then de-paraffinized, quenched for endogenous peroxidase activity with 3% H_2O_2 in methanol for 20 min, and rehydrated. Sections were post-fixed with 4% formalin, and washed with phosphate buffered saline (PBS) containing 0.075 μg/mL glycine (PBSG). Antigens were retrieved with citrate buffer (0.01 M, pH 6.0) at 70 °C for 10 min, followed by incubation in 0.075 g/mL trypsin in PBS at 37 °C for 7 min.

Next, the sections were pre-incubated with 10% normal donkey serum (NDS) in PBS-G. Primary antibodies F4/80 (AbD Serotec), GR-1 (Acris), α-SMA (Sigma-Aldrich) were diluted in 2% NDS in PBSG and incubated over-night at 4 °C. After washing with PBSG, sections were incubated for 60 min with peroxidase labeled secondary antibody against rat (DAKO). After extensive washing with PBSG, diaminobenzidine (DAB) staining was performed for 10 min. After rinsing with water, staining was intensified with Cu_2SO_4 in 0.9% NaCl and rinsed with water again. Finally, the nuclei were counterstained with haematoxylin for 10 s and sections were rinsed for 10 min in water, dehydrated and embedded in distyrene plasticizer xylene (DPX).

Immunoreactivity was evaluated by scoring the wounds. For the F4/80 and GR-1 staining, a single representative section from the centre of each wound (which was selected based on HE stainings) was semi-quantitatively scored according to the following scale: 0 (absent), 1 (mild), 2 (moderate), 3 (marked), 4 (high), 5 (almost exclusively). For the αSMA staining we distinguished the αSMA positive blood vessels that were counted manually and the αSMA-positive myofibroblasts that were scored semi-quantitatively as described with the above scale. All histological sections were recorded using a Zeiss Imager Z1 equipped with an AxioCam MRc5 camera and AxioVision V4.6.3. software (Carl Zeiss Microimaging GmbH, Göttingen, Germany). HE and immuno-stainings (GR-1, F4/80 and αSMA) were imaged at 200x zoom and stitched together using MosaiQ plugin. AZAN stainings were imaged at 100x zoom and stitched together in a similar fashion for quantitative analysis; in addition two representative sections were imaged at 200x zoom to display the finely organized collagenous structures in detail.

2.7. Quantification of collagen formation

AZAN-stained sections were analyzed using ImageJ, by first drawing a 0.25 mm^2 area directly centered on the wound repair tissue. RGB color images received a threshold to isolate blue signal (Hue 120–185, Saturation 0–255, Brightness 0–255). Total tissue area was calculated by applying a threshold that excluded all white (background) signal (Hue 0–255, Saturation 0–255, Brightness 0–254). The blue stained area was then taken as a percentage of the total amount of tissue within the designated area, in order to obtain the total amount of collagen as percentage of tissue area ('collagen expression').

$$\frac{(Total\ area\ \times Collagen\ percentage)}{Tissue\ area} \times 100\% = Collagen\ Expression\ (as\ \%\ of\ tissue\ area)$$

2.8. Statistical analysis

The analysis on development of the relative wound size over time is done as follows: for each mouse the size of the wound at day i (i = 1.7), divided by the size at day 0. A multilevel regression model with a random intercept is used to account for the clustering of data within mice. The number of the day and exposure to PIC and PIC-RGD were used as independent variables. Extension of the model to allow for a non-linear relation is considered, but only if the improvement of the model as expressed in a better likelihood ratio is statistically significant. The software used is R (version 3.4.0) and the lme4 package (version 1.1–13). The histological measurements, namely epithelial migration, granulocyte influx, macrophage influx, myofibroblast population, blood vessel population, and collagen deposition, were analyzed with linear regression analysis. For each of these measurements three models were compared: in the first model, the factors time and presence of gel were tested. In the second model, the presence of RGD side-groups on the PIC gel was added to the analysis. In the third model, the interaction effect of time with both blank PIC gel and PIC-RGD gel was added. Adjusted R^2 values were compared to select the most optimal for each parameter. Significant differences were identified using a p value of 0.05 in the most optimal method.

3. Results

3.1. Matrigel® treated wounds heal normally

In a pilot experiment we first set up a full-thickness excisional wound model with a widely used thermosensitive hydrogel material (Matrigel®). The tissue of 3 and 7 day old wounds and control skin were investigated using HE and AZAN stains (see Supplementary Fig. 2). No morphological differences could be observed between controls and Matrigel® covered wounds. We did detect traces of Matrigel® in the wound area under the crust 3 days after wounding, but not on day 7. All wounds showed expected levels of inflammation for their specific time points and there was no indication that Matrigel® could have induced or reduced inflammation. Lastly, we did not observe any change in animal behavior.

3.2. PIC and PIC-RGD hydrogels do not hamper wound closure

Based on our experience obtained with the pilot we decided to apply the PIC gels in separate animals instead of having the control and PIC hydrogel on wounds of the same animal. Next, we investigated the effects of the PIC hydrogels on wound repair because of its promising intrinsic properties. The PIC and PIC-RGD gel have very similar physical properties and are summarized in Table 1 (see also Supplementary Fig. 3). Both materials were easy to apply to the wounds using a syringe. The ice-cold PIC solutions gelated *in situ* within seconds upon contact with the warm wounded skin. Photographs of the healing wounds were taken and analysed every day up until sacrifice at day 7 (Fig. 1). All wounds neared complete closure around day 7, leaving little to no visible scab or scar. No signs of increased animal stress or excessive scarring were observed. However, one wound treated for 7 days with PIC gel was excluded from the measurements because it was incorrectly angled during histological sectioning. In addition, the abnormally high biological parameters in this section (primarily granulocyte infiltration) were indicative of an infection.

Right after application on day 0, both types of PIC gel are clearly identifiable as droplets on the wounds (see Fig. 1). After 24 h, the droplets' size was reduced and only a thin film layer remained inside the full-thickness defect. As the wounds close, the PIC gels become increasingly more difficult to identify by eye. At day 3, the wounds treated with the PIC-RGD gel seemed more whitish when compared to the PIC gel or control, while most wounds showed no indication of gel presence by day 4.

The effects of the PIC and PIC-RGD on wound closure and the different phases of wound repair were analysed. Wound size was not significantly ($p > 0.05$) affected by addition of the PIC or PIC-RGD gel on any day when compared to control wounds (see Fig. 1). This rules out that the PIC gels, in the present density/concentration, act as a splint and interfere with wound closure. Furthermore, no differences in ease of application, adherent strength, or rate of wound close were detected between PIC and PIC-RGD gels. An overview of the statistical analyses is given in Supplementary Table 1.

3.3. PIC hydrogels do not elicit cytotoxic or excessive inflammatory effects

Possible differences in general histological wound morphology were examined with H&E staining (Fig. 2). On day 3 (Fig. 2, panel A and C) the early inflammatory phase of wound repair is apparent. The scab is large and occupies a considerable part of the wound

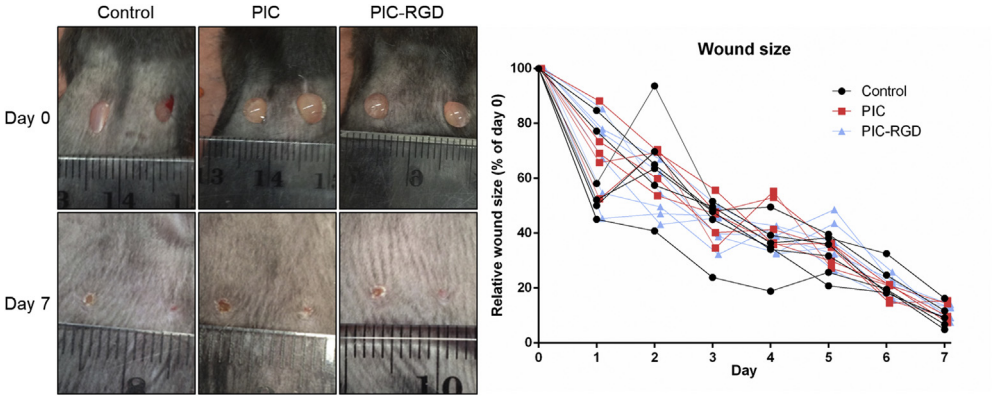

Fig. 1. Topical appearance of the wounds on day 0 and day 7 for control, PIC, and PIC-RGD treated mice. The rate of wound closure is very quick, and some wounds are almost completely closed at day 7. The graph shows the size of the wounds, expressed as percentage of their size at day 0, and reveals that there is no significant difference ($p > 0.05$) in wound closure rate between control and treatment groups.

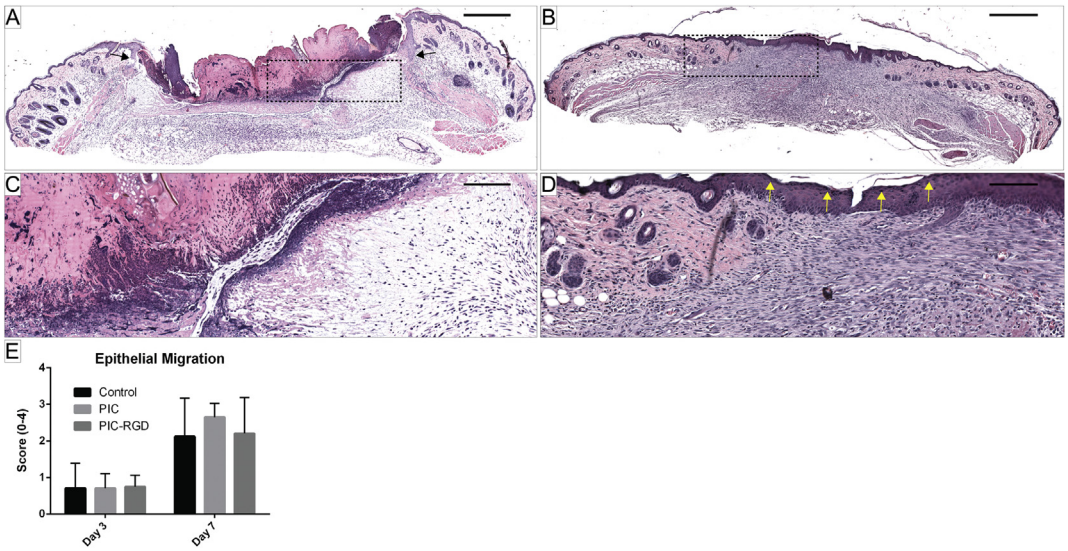

Fig. 2. General H&E staining of PIC-RGD treated wounds and surrounding tissue at day 3 (panel A and C) and day 7 (panel B and D) post-surgery. The area indicated by a dashed box in panels A and B are shown at higher magnification in panels C and D, respectively. Differences in scab size and deposition of wound repair tissue are evident between time points. The migration of epithelium was scored and is displayed in panel E. Control, PIC and PIC-RGD treated wounds appear similar structure-wise. Black scale bar represents 500 μm (panel A and B) and 125 μm (panel C and D). Black arrows (panel A) indicate the newly migrating epithelial edges. Yellow arrows (panel D) point out the keratinization (darker staining) of the upper epithelial layers in the closed wound on day 7, which is characterized by the change in cell shape and shedding of dead cells.

area. The epithelium can be observed migrating from one wound edge to the other below the scab. Deeper wound tissue appears unorganized and unstructured. On day 7 we observed that wound repair has made considerable advancement (Fig. 2, panel B and D). No distinct differences in general morphology of the wounds were detected between control wounds and PIC or PIC-RGD treated wounds. The scab had mostly disappeared and a thick epithelial layer had formed between the wound edges. The wound tissue was considerably denser, suggesting high proliferation and infiltration rates of cells. The fatty and muscle layers (stained in red) were still absent in the wound bed, and both layers end abruptly at the edges of the wound. It is evident that the wound repair is still active and remodelling of the wound is yet to occur. The migration of epithelial cells and subsequent keratinization was scored on a scale of 0–4 (Fig. 2, panel E). In most control and gel-treated wounds epithelial migration started already on day 3, as was apparent from the epithelial edges migrating into the area below the scab. On day 7, the scabs had disappeared or were considerably reduced in size in most cases and coincidentally displayed complete epithelial migration. Keratinization was also observed to have started or already completed in nearly every wound with completed epithelial migration. Statistical analysis showed a significant progression in epithelial migration on day 7 compared to 3 ($p < 0.001$) but no difference between control wounds and those treated with PIC or PIC-RGD gel ($p = 0.543$).

The local tissue's response to the PIC and PIC-RGD gels was analyzed by assessing the number of giant cells, indicative of foreign body reactions, in the wound area 3 days and 7 days after injury. After thorough analysis of H&E sections no giant cells were detected in the wounds at either time point for both treatments as well as the control group (Fig. 2).

Although no giant cells are present during wound repair at days 3 and 7, possible toxic effects of the hydrogel could be related to an exaggerated inflammatory reaction. For this reason, we studied the effects of the gels on the recruitment of both granulocytes and macrophages (Figs. 3 and 4, respectively). Using immunohistochemical analysis, it was demonstrated that at day 3 after injury a strong increase in granulocyte influx was found in the wounds (Fig. 3). A significant decrease in this granulocyte population was found on day 7 compared to day 3 ($p < 0.001$) as expected. Interestingly, the presence of PIC gels appears to significantly decrease granulocyte populations compared to control ($p = 0.003$). The addition of RGD side-groups did not appear to influence granulocytes further.

Next, we investigated possible effects of the hydrogels on F4/80-positive macrophage recruitment using immuno-histochemical analysis (Fig. 4). A clear influx of macrophages was observed at day 3 that further increased on day 7 following excisional injury ($p = 0.036$). No time dependent effect of PIC or PIC-RGD was observed. However, the RGD side groups may play a significant role in macrophage population ($p = 0.018$), as on day 3 the PIC-RGD treated wounds display a higher macrophage population compared to the PIC treated wounds, and this effect inverses on day 7. The statistical analyses for both granulocytes and macrophages are summarized in Supplementary Table 1.

3.4. Myofibroblasts, angiogenesis, and collagen formation are not influenced by PIC hydrogels

To track the presence of myofibroblasts the immunohistological marker αSMA was employed (Fig. 5). No myofibroblasts were observed in any group 3 days after wounding (see Fig. 5 panels A, C, and E). Seven days after injury fibroblasts had differentiated into myofibroblasts ($p < 0.001$) and made up a considerable part of the cell population (Fig. 5 panels B, D, and E). However, the presence of PIC and/or PIC-RGD gel did not significantly alter the levels of myofibroblasts in comparison to the control group on either day 3 or 7 ($p = 0.253$). To assess possible effects of the PIC and PIC-RGD gel on angiogenesis, we counted the number of αSMA-positive blood vessels in the skin following wounding (Fig. 5 panel F). Comparable levels of blood vessels were counted in all samples, indicating no difference between day 3 and 7 ($p = 0.128$) as well as between control group and PIC gels ($p = 0.443$).

In order to analyse the quantity and distribution of collagen in the healing wounds, AZAN staining was performed to distinguish connective tissue/collagen (blue) from other structures (red)

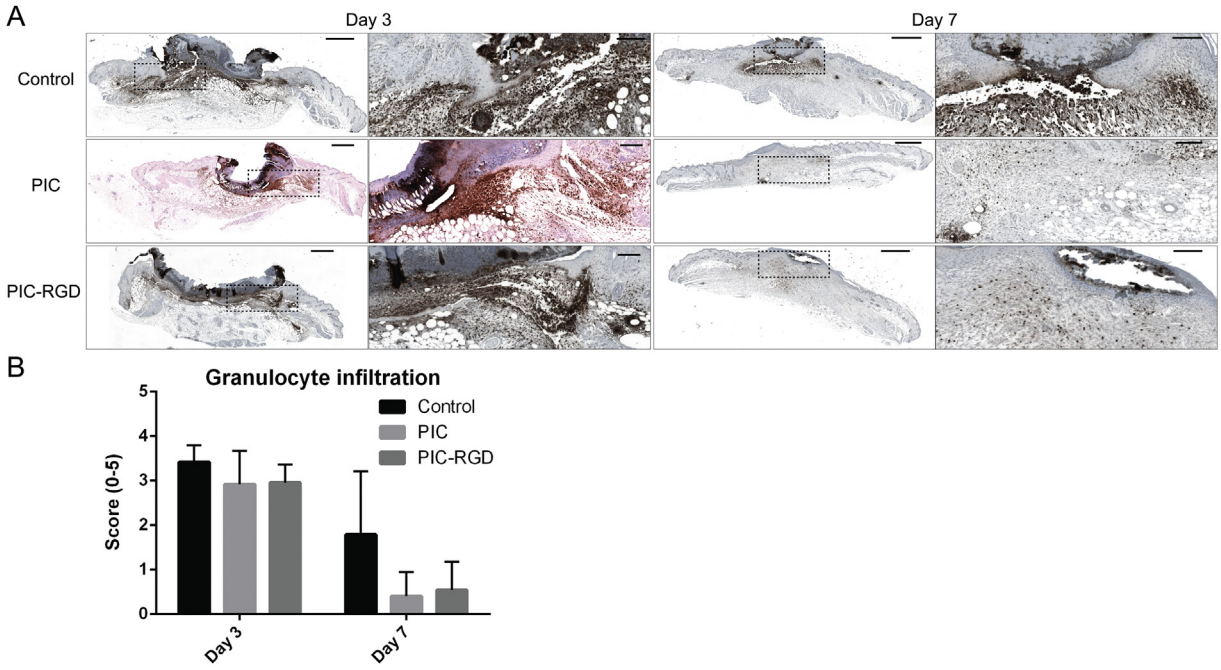

Fig. 3. Immuno-histological staining for granulocyte marker GR-1 (panel A). For sections from day 3 and 7 the left panel is an overview and the right panel represents the dashed box from the left panel at a higher magnification. Cells expressing the granulocyte marker display brown colouring. The infiltration of these cell types was scored and summarized (mean ± SD) in the graph (panel B). Granulocyte population is reduced on day 7 compared to 3 ($p < 0.001$) and for gel treated groups ($p = 0.003$). The black scale bar represents 500 μm in overview panels and 125 μm in high magnification panels.

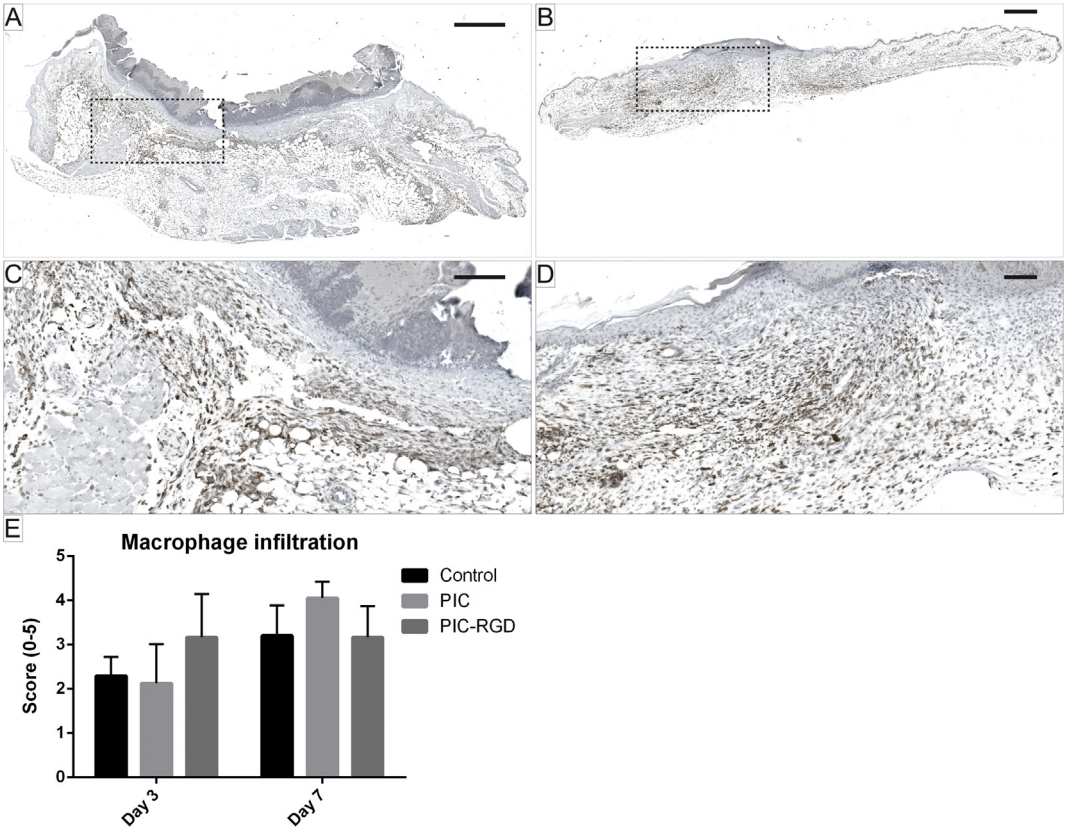

Fig. 4. Immuno-histological staining for macrophage marker F4/80 on day 3 (panels A and C) and day 7 (panel B and D) for PIC-RGD treated wounds. The dashed boxes in panel A and B represent the areas of higher magnification that are displayed in panel C and D, respectively. Cells expressing the macrophage marker display brown colouring. The infiltration of these cell types was scored and summarized (mean ± SD) in the graph (panel E). The black scale bar represents 500 μm in panels A and B and 125 μm in panels C and D.

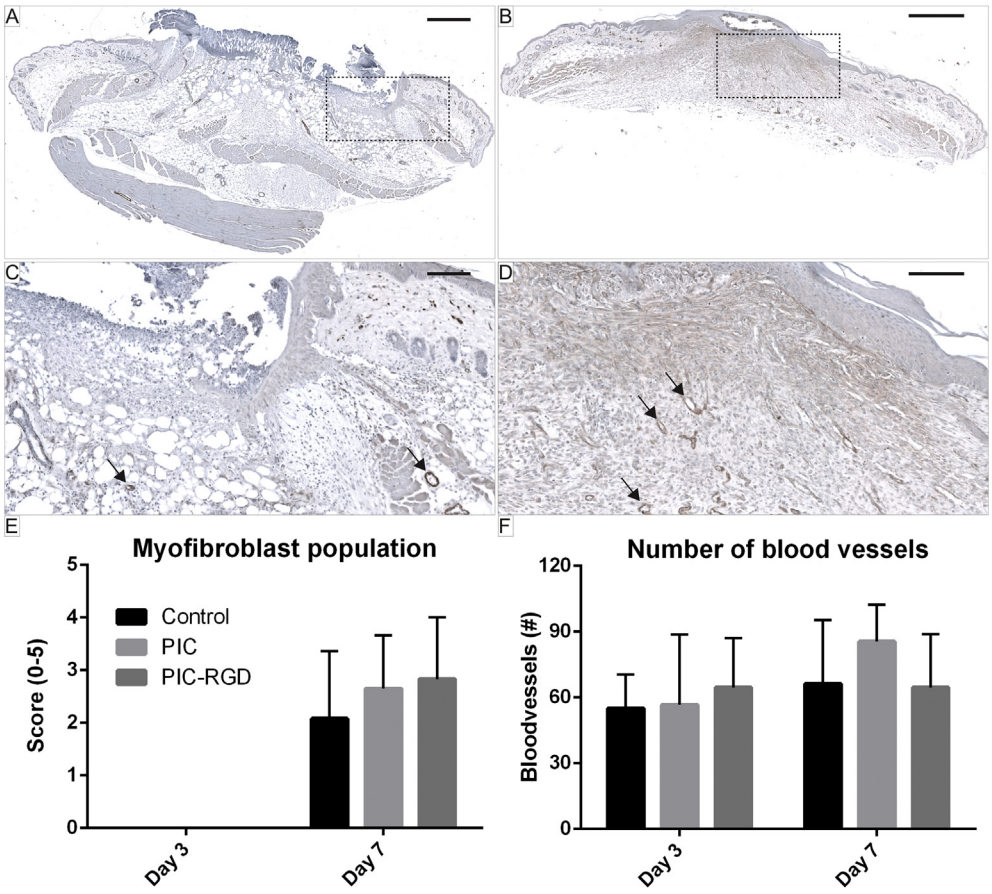

Fig. 5. Immuno-histological staining for myofibroblast marker αSMA (panels A, B, C and D). The dashed boxes in panel A and B represent the areas of higher magnification that are displayed in panel C and D, respectively. Cells expressing αSMA display brown colouring and includes both myofibroblasts and muscle tissue. The infiltration by αSMA expressing myofibroblasts was scored and summarized (mean ± SD) in a graph (panel E). Furthermore, the smooth muscle lining of blood vessels expresses αSMA (indicated by black arrows), allowing for counting of the number of blood vessels in the wound samples (panel F). Black scale bar represents 500 μm in panels A and B and 125 μm in panels C and D.

(Fig. 6). Collagen is typically produced in large quantities once the proliferation phase is initiated. As expected, newly formed collagen was mostly absent in day 3 samples. However, in the 7 day samples the blue stained collagen was produced in the dense wound repair tissue. When comparing this newly deposited collagen to that of the connective tissue of the healthy skin sections, it is apparent that the newly deposited collagen was less intense, sparser and less organized. To determine the contribution of collagen in wound repair tissue in more detail, representative wound areas were selected in each sample. The percentage of blue signal (corresponding to collagen) was quantified using ImageJ software (Fig. 6 panel E). Collagen levels were significantly higher in wound tissue on day 7 compared to 3 ($p < 0.001$). However, since the standard deviation is high on day 7, no significant difference was found when comparing collagen deposition in control wounds and wounds treated with PIC and/or PIC-RGD gel ($p = 0.218$). The results of the statistical analyses for the myofibroblasts, blood vessels, and collagen can be found in Supplementary Table 1.

4. Discussion

In this study, the suitability of the novel PIC thermogel as a wound dressing was investigated in a full-thickness wound model in mice. The administration of PIC and RGD-functionalized-PIC gel to wounds, as well as its effect on wound closure, the short-term biocompatibility, and the inflammatory and proliferative phases of wound repair were investigated.

Pilot experiments with Matrigel® demonstrated that this hydrogel readily gelates upon application on the warm skin of mice. Unfortunately, Matrigel® is an undefined gelatinous protein mixture derived from mouse sarcoma cells, suffering from batch-to-batch variability (including differential expression of cytokines and growth factors) and variability in outcome, which severely limits its clinical translational potential.

Since the synthetic PIC hydrogel offers significant advantages over Matrigel®, we first confirmed that the PIC and PIC-RGD liquid gelated rapidly upon contact with the warm wounded skin of the mice. Next, we demonstrated that the PIC gel with or without RGD sequence did not interfere with wound closure, ruling out that, in the used concentrations of the gel, they could act as a splint. However, it must be considered that the muscle-controlled contraction of skin wounds in mice may overrule any potential effect by the PIC gel. It would be interesting to understand whether different densities of the gel would result in other outcomes. We focussed next on identification of potential negative cytotoxic responses from the material, as well as gaining exploratory insights in the effects of the hydrogel on the different phases of wound repair.

The absence of giant cells in the wound area at days 3 and 7 following application of PIC or PIC-RGD gel suggests that no foreign body reaction was triggered and that biocompatibility in this timeframe was good, albeit this is relatively shortly after the material is placed. This is likely related to the intrinsic properties of the hydrogel mimicking the natural skin micro-environment. The mimicking nature of the gel is supported by previous *in vitro* work

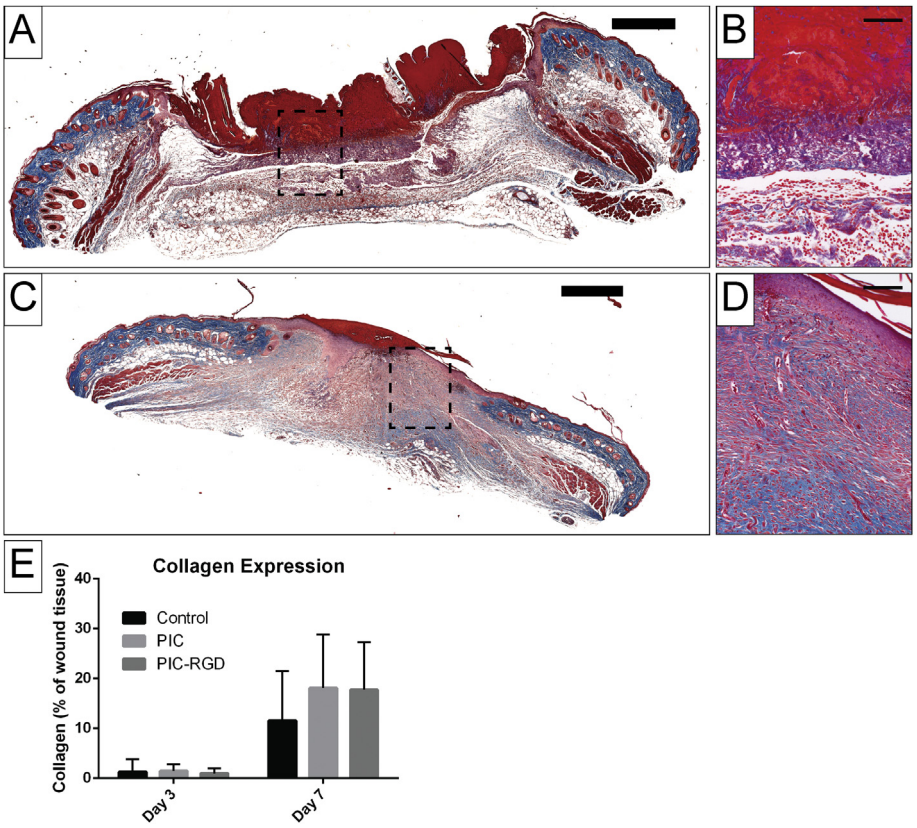

Fig. 6. Histological AZAN staining for collagen (blue) and muscle/nuclei/cytoplasm/erythrocytes (red) in PIC-RGD treated wounds at day 3 (panel A and B) and day 7 (panel C and D). The dashed boxes in panel A and C represent the areas of higher magnification that are displayed in panel B and D, respectively. The percentage of collagen expression (blue signal) in the tissue was calculated with ImageJ and displayed in the graph (mean ± SD) (panel E). Black scale bar represents 500 μm in panels A and C and 100 μm in panels B and D.

[26]. Foreign body type giant cell formation in the dermis in response to synthetic biomaterials are thought to fuel inflammatory processes [36], which could exacerbate wound repair. Migration of epithelium across wound edges was not inhibited or enhanced by treatment with PIC or PIC-RGD gel and occurred in a timely fashion as can be expected from unimpaired full-thickness wounds. Furthermore, we noted that there were no observable differences between wounds treated with the widely used extracellular matrix product Matrigel® and those treated with PIC gel. This implies that PIC gel and Matrigel® have comparable levels of cytocompatibility and that PIC can potentially be a synthetic and more consistent alternative as a replacement matrix.

In the presence of the PIC gels the inflammatory response was not increased, but even attenuated regarding the recruitment of granulocytes on both day 3 and 7. We speculate that this observed decrease in granulocyte recruitment following hydrogel application is related to decreased influx of bacteria. The concentration of the gel dictates the pore size, which is typically between 50 and 150 nm [16,17] and thus should prevent entry by most bacteria as their size typically ranges between 0.1 and 5 μm. It is tempting to speculate that the PIC gel can act as a physical barrier to most pathogens, thus fulfilling one of the most fundamental purposes of a wound dressing. The exposure of wound tissue to bacteria is consequently reduced, attenuating the inflammatory response and allowing for faster resolution of the inflammatory phase. However, one outlier was found in the PIC gel group that demonstrated excessive inflammatory characteristics and was possibly infected. Even if the gel is able to prevent the influx of bacteria, there is still a possibility that bacteria are already inside the wound before the dressing is applied. Noteworthy is that in this study wounds were left open after application of the gel and were thus susceptible to bacterial infiltration from the environment. Addition of antimicrobials to the gel could be a next step of functionalization of the gel to fight off or prevent infection and aid wound repair. Regardless, we cannot confirm this protective effect at this time and must consider also other possibilities, such as a reduction of the GR-1 marker expression over time [38]. Additional *in vivo* or *in vitro* experiments may be able to elucidate whether or not bacteria and mammalian cells are able to penetrate through a PIC gel barrier.

To enter the proliferation phase, resolution of inflammation is necessary. This is characterized by an attenuation of endothelial activation, resulting in diminished leukocyte-endothelial cell interactions and, subsequently, decreased influx of granulocytes to the wound area and attenuated levels of pro-inflammatory cytokines. It is thought that during the wound healing process, first pro-inflammatory M1 macrophages enter the wound site to clear cellular debris and to destroy invading pathogens. Besides pro-inflammatory M1 macrophages, there are various other macrophage subsets, including the anti-inflammatory M2 macrophages and the Mhem, Mox, and M4 macrophages [39–41]. Under the right conditions, M1 macrophages may therefore skew into anti-inflammatory macrophage subsets contributing to resolution of inflammation. It would be interesting to investigate whether the PIC hydrogel can attenuate inflammation by skewing towards an anti-inflammatory macrophage phenotype, with or without conjugated biofunctional molecules [42]. Macrophage levels do not appear to change between day 3 and 7, yet the values of PIC-RGD treated wounds change in comparison to blank PIC treated wounds. On day 3, exposure to blank PIC gels result in less macrophages, whereas on day 7 this effect reverses to an increase. The

implication of this observation is unclear, but may be related to the interaction of macrophages with RGD peptides. As interaction with ECM components can facilitate macrophage differentiation, it is not unlikely that the ECM-mimicking PIC-RGD gels may facilitate this process as well [43]. Currently the impact of RGD-functionalized PIC remains unclear.

Since we did not observe adverse effects of the gel during wound repair, we aim to translate our PIC gel from the preclinical phase to the human setting when our future investigations do not reveal toxic reactions. However, a limitation of our study is that we were not able to verify how long the gel remains on the wound. Moreover, the gel was not visible in the histological sections. After one day already, the gel shrunk to a thin film what could be explained only in part by evaporation or absorption of the saline. We suspect that part of the gel is lost during grooming and later during histological processing. It is important to realise that mice (unlike humans) possess a subcutaneous muscle layer, known as *panniculus carnosus*, that facilitates the closure of wounds. Thus, in upcoming studies we will include a splint to prevent contraction by primary intention (i.e. muscle contraction) as well as a secondary bandage dressing that protects the gel. These conditions better mimic the human process of wound repair, where wound closure is mainly mediated by myofibroblast contraction and epithelial migration, while simultaneously ensuring preservation of the gel inside the wound.

We anticipated that the inclusion of RGD to the side-chains of PIC would enhance biocompatibility by improving the cell-material interaction. However, in this study, no evidence could be obtained to support this hypothesis. Both gels appeared to adhere equally well to the wound macroscopically and had similar mechanical strength, adhesive ability of PIC gel was thus sufficient enough even without the presence of RGD peptide. Although interaction between RGD peptides and macrophages was previously observed to elicit different cytokine patterns [42], it is currently unknown which implications this has *in vivo* and whether or not this involves macrophage phenotype changes. Recent research focused on the optimization of PIC-RGD concentration and molecular structure for 3D cell culture [28]. There it was demonstrated that PIC may facilitate adipogenic differentiation and blood capillary formation *in vitro*. It also highlights that the concentration and available RGD peptides per polymer may have to be carefully calibrated in order to achieve cellular infiltration into the gel.

The novelty of PIC wound dressing must be considered over some of the commonly used products currently in research or used in the clinic. We found that most polymer-based dressings require formation *ex situ* and are often applied in preshaped sheets [44]. In regards to temperature sensitive gel dressings; in the work by Wang et al. a method was investigated to apply a bioactive glass/gelatin composite gel as a spray, rather than a pre-formed gel [45]. The gels were first stirred to form a semi-fluid paste and after application required up to 10 min to restore themselves as a homogenous gel. In terms of speed, the heat-induced gelation of PIC may be considered superior as this process is initiated within seconds and finishes in a minute. After homogenous dissolution the PIC solution can be stored in the fridge and immediately be used when required. Furthermore, recent work has shown that the gelation point of PIC gel can be adjusted to be between 10 and 60 °C, which may allow us to apply and remove the gel at a higher temperature and thus improve patient comfort [46]. Other studies may instead focus on the tuneable delivery of drugs with hydrogels [47,48]. Current in-house research is also focussing on the delivery of encapsulated drugs using PIC hydrogel. So far, these results seem promising and highlight additional options for wound treatment than the covalent binding of functional groups. Regarding biocompatibility many natural products, such as hyaluronic acid dressings, have the advantage of being inherently biocompatible and biodegradable [49]. Furthermore, in the case of hyaluronic acid, its molecular structure was suggested to promote cell migration and proliferation, which may aid in the recruitment of cells necessary for wound repair, and angiogenesis in particular. As another example, Chitosan-based dressings offer similar levels of biocompatibility while simultaneously providing inherent antimicrobial activities. Previously, thermo-responsive hydrogels based on chitosan and agarose were already shown to enhance healing, prevent infection, and alter the pattern of re-epithelialization [50]. These kinds of studies illustrate the potential for hydrating wound dressings that are convenient to apply. In another study [37], biodegradable gel (that was partially based on PEG) could outperform untreated wounds as well as wounds treated with an over-the-counter wound dressing (NewSkin®) and clinically used Aquacel® and Aquacel Ag® [51] for dermal maturation, fibroblast infiltration, and collagen synthesis in full-thickness murine skin wounds. We included in our study the same analysis method for epithelial migration but observed that epithelial migration already reached stage 2 or 3 (complete migration with partial or complete keratinization) on day 7 while wounds from that study were still in stage 1 (partial migration). This can be explained by the initial wound size, which was 15 mm in their study and only 4 mm in ours, and is thus important for the interpretation of such results. Regardless, the authors mention that the degradability of their material helped in preventing embedment in deeper tissues, which can potentially lead to long-term complications. How the high stability of the PIC polymer influences long-term compatibility remains to be discovered.

Ultimately, it has become apparent that PIC can perform on-par with some of the currently used products with its main strengths being ease of application, hydration, and potential for functionalization. Other properties, such as strain stiffening, pore size, and convenient chemical modifiability require further investigation to determine how these may be manipulated to benefit wound healing. Since matrix mechanics are becoming an indispensable part of the ECM and wound repair, the biomimetic synthetic PIC-hydrogel may possibly replace wound dressings based on natural materials such as collagen or fibrin.

5. Conclusions

In our study we observed that the *in situ* gelating PIC hydrogel acts as a novel wound dressing, without adverse effects, and offering simultaneous ease of application among other beneficial characteristics. PIC hydrogels gelate upon contact with body heat, and stay adherent to the wound without additional support. The gels have the potential for mechanical optimization as well as the delivery of therapeutic drugs such as antibiotics, which combined with the mesoporous structure, may offer a very effective anti-inflammatory action. Research is currently ongoing to further develop PIC gel into a usable wound dressing that can easily and painlessly be applied and removed without disturbance of wound repair. Specifically, further development is focussed on the application in large and complicated wounds such as those of burn patients.

Data availability

The raw/processed data required to reproduce these findings cannot be shared at this time due to technical or time limitations.

Acknowledgements and conflict of interest

This study was supported by grants from EFRO (Flowplast

#2013-014760) and ZONMW (Biomimetic Hydrogel allowing customizable Wound Care #436001005). We want to thank René E.M. van Rheden for expert advice on immuno-histochemical stainings. AER has several patents regarding the preparation use of the PIC gel (#EP2287221, EP3021872, WO2017037293). AER holds shares in Noviotech BV, and owns patent rights for PIC gel and GRGDS conjugates (EP3021872B1).

Appendix A. Supplementary data

Supplementary data related to this article can be found at https://doi.org/10.1016/j.biomaterials.2018.07.038.

References

[1] F.A. Wagener, A. Scharstuhl, R.M. Tyrrell, J.W. Von den Hoff, A. Jozkowicz, J. Dulak, et al., The heme-heme oxygenase system in wound healing; implications for scar formation, Curr. Drug Targets 11 (2010) 1571–1585.
[2] D.M. Lundvig, S. Immenschuh, F.A. Wagener, Heme oxygenase, inflammation, and fibrosis: the good, the bad, and the ugly? Front. Pharmacol. 3 (2012) 81.
[3] F.A. Wagener, H.D. Volk, D. Willis, N.G. Abraham, M.P. Soares, G.J. Adema, et al., Different faces of the heme-heme oxygenase system in inflammation, Pharmacol. Rev. 55 (2003) 551–571.
[4] F.A. Wagener, H.E. van Beurden, J.W. von den Hoff, G.J. Adema, C.G. Figdor, The heme-heme oxygenase system: a molecular switch in wound healing, Blood 102 (2003) 521–528.
[5] S. Dhivya, V.V. Padma, E. Santhini, Wound dressings - a review, Biomedicine 5 (2015) 22.
[6] A. Sood, M.S. Granick, N.L. Tomaselli, Wound dressings and comparative effectiveness data, Adv. Wound Care 3 (2013) 511–529.
[7] A. Jones, D. Vaughan, Hydrogel dressings in the management of a variety of wound types: a review, J. Orthop. Nurs. 9 (Supplement 1) (2005) S1–S11.
[8] T.P. Amadeu, A.B. Seabra, M.G. De Oliveira, A.M.A. Costa, S-nitrosoglutathione-containing hydrogel accelerates rat cutaneous wound repair, J. Eur. Acad. Dermatol. Venereol. 21 (2007) 629–637.
[9] J.L. Georgii, T.P. Amadeu, A.B. Seabra, M.G. de Oliveira, A. Monte-Alto-Costa, Topical S-nitrosoglutathione-releasing hydrogel improves healing of rat ischaemic wounds, J. Tissue Eng. Regenerative Med. 5 (2011) 612–619.
[10] C.Y. Gong, Q.J. Wu, Y.J. Wang, D.D. Zhang, F. Luo, X. Zhao, et al., A biodegradable hydrogel system containing curcumin encapsulated in micelles for cutaneous wound healing, Biomaterials 34 (2013) 6377–6387.
[11] D. Choi, S. Kim, Y.-M. Lim, H.-J. Gwon, J. Park, Y.-C. Nho, et al., Hydrogel incorporated with chestnut honey accelerates wound healing and promotes early HO-1 protein expression in diabetic (db/db) mice, Tissue Eng. Regen. Med. 9 (2012) 36–42.
[12] A. Song, A.A. Rane, K.L. Christman, Antibacterial and cell-adhesive polypeptide and poly(ethylene glycol) hydrogel as a potential scaffold for wound healing, Acta Biomater. 8 (2012) 41–50.
[13] V.W. Wong, K.C. Rustad, J.P. Glotzbach, M. Sorkin, M. Inayathullah, M.R. Major, et al., Pullulan hydrogels improve mesenchymal stem cell delivery into high-oxidative-stress wounds, Macromol. Biosci. 11 (2011) 1458–1466.
[14] M. Jaspers, S.L. Vaessen, P. van Schayik, D. Voerman, A.E. Rowan, P.H.J. Kouwer, Nonlinear mechanics of hybrid polymer networks that mimic the complex mechanical environment of cells, Nat. Commun. 8 (2017) 15478.
[15] M. Jaspers, M. Dennison, M.F.J. Mabesoone, F.C. MacKintosh, A.E. Rowan, P.H.J. Kouwer, Ultra-responsive soft matter from strain-stiffening hydrogels, Nat. Commun. 5 (2014) 5808.
[16] P.H. Kouwer, M. Koepf, V.A. Le Sage, M. Jaspers, A.M. van Buul, Z.H. Eksteen-Akeroyd, et al., Responsive biomimetic networks from polyisocyanopeptide hydrogels, Nature 493 (2013) 651–655.
[17] M. Jaspers, A.C.H. Pape, I.K. Voets, A.E. Rowan, G. Portale, P.H.J. Kouwer, Bundle formation in biomimetic hydrogels, Biomacromolecules 17 (2016) 2642–2649.
[18] R. Agha, R. Ogawa, G. Pietramaggiori, D.P. Orgill, A review of the role of mechanical forces in cutaneous wound healing, J. Surg. Res. 171 (2011) 700–708.
[19] B. Hinz, Tissue stiffness, latent TGF-β1 Activation, and mechanical signal transduction: implications for the pathogenesis and treatment of fibrosis, Curr. Rheumatol. Rep. 11 (2009) 120.
[20] U. Hersel, C. Dahmen, H. Kessler, RGD modified polymers: biomaterials for stimulated cell adhesion and beyond, Biomaterials 24 (2003) 4385–4415.
[21] E. Ruoslahti, RGD and other recognition sequences for integrins, Annu. Rev. Cell Dev. Biol. 12 (1996) 697–715.
[22] M.D. Pierschbacher, E. Ruoslahti, Cell attachment activity of fibronectin can be duplicated by small synthetic fragments of the molecule, Nature 309 (1984) 30–33.
[23] K.S. Tweden, H. Harasaki, M. Jones, J.M. Blevitt, W.S. Craig, M. Pierschbacher, et al., Accelerated healing of cardiovascular textiles promoted by an RGD peptide, J. Heart Valve Dis. 4 (Suppl 1) (1995) S90–S97.
[24] P.M. Mertz, S.C. Davis, L. Franzen, F.D. Uchima, M.P. Pickett, M.D. Pierschbacher, et al., Effects of an arginine-glycine-aspartic acid peptide-containing artificial matrix on epithelial migration in vitro and experimental second-degree burn wound healing in vivo, J. Burn Care Rehabil. 17 (1996) 199–206.
[25] S. Mandal, Z.H. Eksteen-Akeroyd, M.J. Jacobs, R. Hammink, M. Koepf, A.J.A. Lambeck, et al., Therapeutic nanoworms: towards novel synthetic dendritic cells for immunotherapy, Chem. Sci. 4 (2013) 4168–4174.
[26] R.K. Das, V. Gocheva, R. Hammink, O.F. Zouani, A.E. Rowan, Stress-stiffening-mediated stem-cell commitment switch in soft responsive hydrogels, Nat. Mater. 15 (2016) 318–325.
[27] S.R. Deshpande, R. Hammink, R.K. Das, F.H.T. Nelissen, K.G. Blank, A.E. Rowan, et al., Dna-responsive polyisocyanopeptide hydrogels with stress-stiffening capacity, Adv. Funct. Mater. 26 (2016) 9075–9082.
[28] J. Zimoch, J.S. Padial, A.S. Klar, Q. Vallmajo-Martin, M. Meuli, T. Biedermann, et al., Polyisocyanopeptide hydrogels: a novel thermo-responsive hydrogel supporting pre-vascularization and the development of organotypic structures, Acta Biomater. 70 (2018) 129–139.
[29] J.J. Cornelissen, J.J. Donners, R. de Gelder, W.S. Graswinckel, G.A. Metselaar, A.E. Rowan, et al., Beta -Helical polymers from isocyanopeptides, Science 293 (2001) 676–680.
[30] M. Koepf, H.J. Kitto, E. Schwartz, P.H.J. Kouwer, R.J.M. Nolte, A.E. Rowan, Preparation and characterization of non-linear poly(ethylene glycol) analogs from oligo(ethylene glycol) functionalized polyisocyanopeptides, Eur. Polym. J. 49 (2013) 1510–1522.
[31] N. Cremers, D. Lundvig, S. van Dalen, R. Schelbergen, P. van Lent, W. Szarek, et al., Curcumin-induced heme Oxygenase-1 expression prevents H2O2-Induced cell death in wild type and heme Oxygenase-2 knockout adipose-derived mesenchymal stem cells, Int. J. Mol. Sci. 15 (2014) 17974.
[32] D.M.S. Lundvig, A. Scharstuhl, N.A.J. Cremers, S.W.C. Pennings, J. te Paske, R. van Rheden, et al., Delayed cutaneous wound closure in HO-2 deficient mice despite normal HO-1 expression, J. Cell Mol. Med. 18 (2014) 2488–2498.
[33] C.A. Schneider, W.S. Rasband, K.W. Eliceiri, NIH Image to ImageJ: 25 years of image analysis, Nat. Methods 9 (2012) 671.
[34] P.L. Carvajal Monroy, S. Grefte, A.M. Kuijpers-Jagtman, M.P. Helmich, F.A. Wagener, J.W. Von den Hoff, Fibrosis impairs the formation of new myofibers in the soft palate after injury, Wound Repair Regen. 23 (2015) 866–873.
[35] P.L. Carvajal Monroy, S. Grefte, A.M. Kuijpers-Jagtman, F.A. Wagener, J.W. Von den Hoff, Strategies to improve regeneration of the soft palate muscles after cleft palate repair, Tissue Eng. B Rev. 18 (2012) 468–477.
[36] W.J. Kao, A.K. McNally, A. Hiltner, J.M. Anderson, Role for interleukin-4 in foreign-body giant cell formation on a poly(etherurethane urea) in vivo, J. Biomed. Mater. Res. 29 (1995) 1267–1275.
[37] C.C. Yates, D. Whaley, R. Babu, J. Zhang, P. Krishna, E. Beckman, et al., The effect of multifunctional polymer-based gels on wound healing in full thickness bacteria-contaminated mouse skin wound models, Biomaterials 28 (2007) 3977–3986.
[38] J.M. Daley, S.K. Brancato, A.A. Thomay, J.S. Reichner, J.E. Albina, The phenotype of murine wound macrophages, J. Leukoc. Biol. 87 (2010) 59–67.
[39] T.D. Hull, A. Agarwal, J.F. George, The mononuclear phagocyte system in homeostasis and disease: a role for heme Oxygenase-1, Antioxidants Redox Signal. 20 (2014) 1770–1788.
[40] D.A. Chistiakov, Y.V. Bobryshev, A.N. Orekhov, Changes in transcriptome of macrophages in atherosclerosis, J. Cell Mol. Med. 19 (2015) 1163–1173.
[41] H.J. Medbury, H. Williams, J.P. Fletcher, Clinical significance of macrophage phenotypes in cardiovascular disease, Clin. Transl. Med. 3 (2014) 63.
[42] M. Bartneck, H.A. Keul, M. Wambach, J. Bornemann, U. Gbureck, N. Chatain, et al., Effects of nanoparticle surface-coupled peptides, functional endgroups, and charge on intracellular distribution and functionality of human primary reticuloendothelial cells, Nanomedicine 8 (2012) 1282–1292.
[43] S.S. Jacob, P. Shastry, P.R. Sudhakaran, Monocyte-macrophage differentiation in vitro: modulation by extracellular matrix protein substratum, Mol. Cell. Biochem. 233 (2002) 9–17.
[44] E.A. Kamoun, E.-R.S. Kenawy, X. Chen, A review on polymeric hydrogel membranes for wound dressing applications: PVA-based hydrogel dressings, J. Adv. Res. 8 (2017) 217–233.
[45] C. Wang, F. Zhu, Y. Cui, H. Ren, Y. Xie, A. Li, et al., An easy-to-use wound dressing gelatin-bioactive nanoparticle gel and its preliminary in vivo study, J. Mater. Sci. Mater. Med. 28 (2016) 10.
[46] P.H.J. Kouwer, P. de Almeida, O. ven den Boomen, Z.H. Eksteen-Akeroyd, R. Hammink, M. Jaspers, et al., Controlling the gelation temperature of biomimetic polyisocyanides, Chin. Chem. Lett. 29 (2018) 281–284.
[47] C. Ma, Y. Shi, D.A. Pena, L. Peng, G. Yu, Thermally responsive hydrogel blends: a general drug Carrier model for controlled drug release, Angew. Chem. 127 (2015) 7484–7488.
[48] J. Henise, B.R. Hearn, G.W. Ashley, D.V. Santi, Biodegradable tetra-PEG hydrogels as carriers for a releasable drug delivery system, Bioconjugate Chem. 26 (2015) 270–278.
[49] C.W.Y. John, dA. Giovanni, Functions of hyaluronan in wound repair, Wound Repair Regen. 7 (1999) 79–89.
[50] S.P. Miguel, M.P. Ribeiro, H. Brancal, P. Coutinho, I.J. Correia, Thermoresponsive chitosan–agarose hydrogel for skin regeneration, Carbohydr. Polym. 111 (2014) 366–373.
[51] Y. Barnea, J. Weiss, E. Gur, A review of the applications of the hydrofiber dressing with silver (Aquacel Ag(®)) in wound care, Therapeut. Clin. Risk Manag. 6 (2010) 21–27.